

Heat capacity and thermal conductivity of multiferroics $\text{Bi}_{1-x}\text{Pr}_x\text{FeO}_3$

S. N. Kallaev^a, Z. M. Omarov^a, R.G. Mitarov^b, S. A. Sadykov^c, S. V. Khasbulatov^d, L. A. Reznichenko^d, K. Bormanis^e, and M. Kundzinsh^e

^aDagestan Science Centre, Institute of Physics, RAS, Makhachkala, Russia; ^bDagestan State Technical University, Makhachkala, Russia; ^cPhysical Department, Dagestan State University, Makhachkala, Russia; ^dSouthern Federal University, Rostov on Don, Russia; ^eInstitute of Solid State Physics, University of Latvia, Riga, Latvia

ABSTRACT

The heat capacity and thermal conductivity of multiferroics $\text{Bi}_{1-x}\text{Pr}_x\text{FeO}_3$ ($0 \leq x \leq 0.50$) has been studied in the temperature range of 130–800 K. A slight substitution of praseodymium for bismuth is found to lead to a noticeable shift of the antiferromagnetic phase transition temperature whilst the heat capacity increases. The temperature dependences of the heat capacity and thermal conductivity exhibit additional anomalies during phase transitions. The experimental results suggest that the excess heat capacity can be attributed to the Schottky effect for three-level states. The basic mechanisms of the heat transfer of phonons are highlighted and the dependence of the mean free path on temperature is determined.

ARTICLE HISTORY

Received 2 October 2018
Accepted 8 February 2019

KEYWORDS

Multiferroics; heat capacity; thermal conductivity

1. Introduction

In recent years there has been a surge of researchers' interest in crystal structure and physical properties of multiferroics, i.e. materials characterized by coexistence of magnetic and ferroelectric orderings. Researchers' interest in such materials has been prompted by the potentials of practical applications. Multiferroics can be used to develop magnetic field sensors, data recorder/reader, spinelectronics and microwave ovens and other devices. These promising materials include bismuth ferrite BiFeO_3 , which undergoes the ferroelectric (at $T_c \sim 1083$ K) and the anti-ferromagnetic (at $T_N \sim 643$ K) phase transitions [1]. Bismuth ferrite has space group $R3c$ at room temperature. The crystal structure is characterized by the presence of rhombohedrally distorted perovskite cells approximating the cubic shape. At temperatures below the Néel point T_N , bismuth ferrite exhibits a complex spatially-modulated cycloid-type magnetic structure that does not allow the existence of ferromagnetic properties [2]. A necessary condition for the appearance of the magnetoelectric effect is destruction of its spatially-modulated spin structure that can be obtained by doping the bismuth ferrite with rare-earth elements.

Results of studies of ceramic BiFeO_3 samples modified with rare-earth elements demonstrate some difference of opinions concerning the sequence of structural phase

transitions and the temperature ranges of the existence of different phases with substitutions of various rare-earth elements and with their increased concentration.

The temperature dependence of crystal structure of solid solutions $\text{Bi}_{1-x}\text{Pr}_x\text{FeO}_3$ is different from the structural changes observed in the BiFeO_3 compositions with other rare-earth ions substitution [3, 4]. It was demonstrated [5, 6] that at increasing temperatures the $\text{Bi}_{1-x}\text{Pr}_x\text{FeO}_3$ compositions have a tendency to form a two-phase and three-phase structural states in a certain temperature range, in which the rhombohedral and the orthorhombic phases should coexist. The results encourage further studies of bismuth ferrite based multiferroics doped by rare-earth elements. In particular, the calorimetric measurements over a wide temperature range make it possible to detect anomalies of the heat capacity, yielding important information on the nature of the involved physical phenomena. It is worthwhile to mention, that the heat capacity and thermal conductivity of the $\text{Bi}_{1-x}\text{Pr}_x\text{FeO}_3$ system has not yet been a subject of extensive studies. Earlier in our work [7] the results of studies of the heat capacity of $\text{Bi}_{1-x}\text{Pr}_x\text{FeO}_3$ of some compositions with concentrations $0 \leq x \leq 0.20$ were presented. This study investigates the heat capacity and thermal conductivity of multiferroics $\text{Bi}_{1-x}\text{Pr}_x\text{FeO}_3$ with concentrations $0 \leq x \leq 0.50$ over a wide temperature range 130–800 K.

2. Experimental

Ceramic samples of $\text{Bi}_{1-x}\text{Pr}_x\text{FeO}_3$ solid solutions with $x = 0, 0.05, 0.10, 0.15, 0.20, 0.30, 0.40$ and 0.50 were prepared the popular ceramic technology involving solid-phase synthesis with subsequent sintering in air without additional pressure. The synthesis was performed using high-purity oxides for two stages with intermediate milling and granulating the powders. The synthesis conditions were as follows: the first stage sintering – calcination was at temperature $T_1 = 800^\circ\text{C}$ ($\tau_1 = 10$ h), and the second stage sintering was performed at $T_2 = 800\text{--}850^\circ\text{C}$ ($\tau_2 = 5$ h). A plasticizer with subsequent granulation was introduced into the powder to give it the properties required for pressing. The optimal sintering temperature was chosen in the range $900 \leq T_{\text{ann}} \leq 950^\circ\text{C}$. The X-ray powder diffraction analyses were performed using a DRON-3 diffractometer with FeK_α and CuK_α radiations. Thus prepared solid solutions had fairly high relative (89–94%) densities, which corresponds to the density limits achieved in the common ceramic technology (90–95%) that indicated sufficiently high quality of the ceramics.

The heat capacity was measured using the NETZSCH DSC 204 F1Phoenix® differential scanning calorimeter. The samples were in the form of 1 mm thick plate with 4 mm diameter. The temperature was varied with step 5 K/min. The heat capacity was measured with accuracy 3%.

Studies of thermal diffusivity and thermal conductivity were carried out by laser flash on the LFA-457 MicroFlash unit from NETZSCH. Samples used were 12.5 mm in diameter and 1 mm in thickness. Thermal conductivity was derived by the formula $\lambda = \eta \cdot C_p \cdot \rho$ (where η is the thermal diffusivity, ρ is the density of sample, C_p – heat capacity).

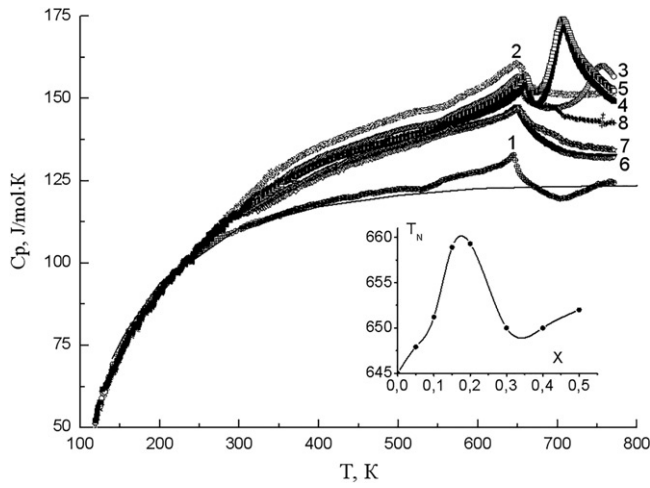


Figure 1. Temperature dependence of heat capacity of $\text{Bi}_{1-x}\text{Pr}_x\text{FeO}_3$ with $x=0$ (1), 0.05 (2), 0.10 (3), 0.15 (4), 0.20 (5), 0.30 (6), 0.40 (7) and 0.50 (8); solid line is shown the result of the approximation of the phonon heat capacity by the Debye function. The inset: T_N - x phase diagram of the $\text{Bi}_{1-x}\text{Pr}_x\text{FeO}_3$ system.

3. Results and discussion

The X-ray phase analysis data show that the impurity-free solid solutions were formed exclusively at the Pr concentration $x \geq 0.12$; at lower x the samples contained low concentration of the $\text{Bi}_{25}\text{FeO}_{40}$ and $\text{Bi}_2\text{Fe}_4\text{O}_9$ compounds. The analysis of the diffraction reflections revealed several concentration ranges with different phase compositions. In the range $0 \leq x < 0.10$, the rhombohedral ($R3c$) phase (inherent to BiFeO_3) was found to exist. Three phases coexisted at $0.10 < x \leq 0.20$: one rhombohedral $R3c$ and two orthorhombic P_1 -type PbZrO_3 and P_2 -type GdFeO_3 (the former phase was dominant). In the range of $0.20 < x \leq 0.30$, phase $R3c$ disappeared, but two phases P_1 and P_2 coexisted. A similar situation was observed during experiments with solid solutions $\text{Bi}_{1-x}\text{La}_x\text{FeO}_3$ [4] and $\text{Bi}_{1-x}\text{Pr}_x\text{FeO}_3$ [5, 6, 8].

Figure 1 shows the heat capacity C_p of $\text{Bi}_{1-x}\text{Pr}_x\text{FeO}_3$ ($x=0, 0.05, 0.10, 0.15, 0.20, 0.30, 0.40$ and 0.50) in the temperature range of 130–800 K. It is apparent (Figure 1) that, the temperature dependences of the heat capacity for all compositions exhibit anomalies near the antiferromagnetic phase transition temperature T_N , and C_p temperature shifts to higher values as x increases ($0 < x \leq 0.20$), whilst T_N tends to lower temperatures in compositions with $x > 0.2$. When BiFeO_3 is substituted by praseodymium the heat capacity increases in a wide temperature ranges above $T \geq 240$ K. The inset in Figure 1 presents the T_N - x phase diagram of the $\text{Bi}_{1-x}\text{Pr}_x\text{FeO}_3$ system plotted basing on results of the heat capacity measurements. The heat capacity vs temperature curves for $x=0.10$, $x=0.15$ and 0.20 exhibit the second anomalies, typical for phase transitions, at temperatures higher than T_N : $T \approx 755$ K and ≈ 710 K, respectively. According to the X-ray diffraction studies of $\text{Bi}_{1-x}\text{Pr}_x\text{FeO}_3$ [5, 6], we can suppose that the heat capacity anomalies at $T \approx 710$ K (Figure 1a) for the compositions with $x=0.15$ and 0.20 could be attributed to the phase transition between the antipolar and nonpolar orthorhombic $Pnma$ and $Pnma$ structures, while the anomalous behavior of the heat capacity for

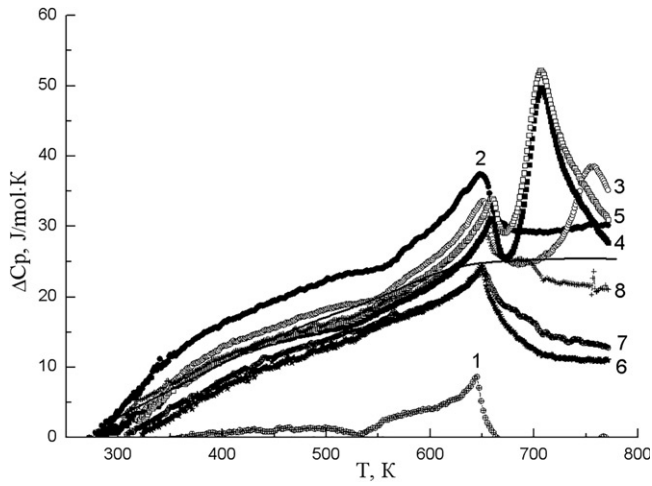


Figure 2. Temperature dependence of the anomalous component of heat capacity of $\text{Bi}_{1-x}\text{Pr}_x\text{FeO}_3$ for $x = 0$ (1), 0.05 (2), 0.10 (3), 0.15 (4), 0.20 (5), 0.30 (6), 0.40 (7) and 0.50 (8); solid line is shown the result of the approximation by Eq. (1).

$x = 0.10$ at $T \approx 755$ K is related to the structural phase transition between rhombohedral $R3c$ and orthorhombic $Pnma$ structures.

The experimental values of heat capacity over a wide temperature range should be analyzed by taking into account the anharmonic contribution to the phonon heat capacity. This component of the heat capacity can be calculated using the experimental data of compressibility K_T and thermal expansion coefficient α ($C_p - C_v = V\alpha^2 T/K_T$, where V is the molar volume). There are no available data on the compressibility of BiFeO_3 , accordingly, the anharmonic contribution to the phonon heat capacity is obtained basing on thermal expansion coefficient measured on $\text{Bi}_{1-x}\text{La}_x\text{FeO}_3$ samples in [9] and the pressure dependence of volume studied for LaAlO_3 [10] with a similar structure. Basing on these data, the anharmonic contribution to the phonon heat capacity of BiFeO_3 at 300 K is found to be about 1 J/mol K, i.e. less than 1% of the total heat capacity. The small anharmonic contribution is due to a fairly low thermal expansion coefficient of BiFeO_3 . The further analysis of the temperature dependence of the phonon heat capacity can be performed whilst the difference between C_p and C_v , can be neglected.

In the most cases, the quantitative analysis of the temperature dependence of heat capacity and separation of the phonon and the anomalous contribution is performed using a simple model, whereby the phonon heat capacity should be governed by the Debye function $C_v^0 \sim D(\Theta_D/T)$, where Θ_D is the Debye characteristic temperature. The calculation procedure yields the heat capacity of BiFeO_3 with the value $\Theta_D \approx 550$ K.

The calculation results of phonon heat capacity of $\text{Bi}_{1-x}\text{Pr}_x\text{FeO}_3$ using the Debye function are indicated in Figure 1 by the solid line. The BiFeO_3 compositions modified with Pr demonstrate the deviations of the experimental points from the calculated phonon heat capacity indicating the existence of the excess heat capacity (Figure 2). The excess component of the heat capacity is found as the difference between the measured C_p and the calculated C_p^0 phonon heat capacity $\Delta C_p = C_p - C_p^0$ (for each composition). The temperature dependence of the anomalous heat capacity $\Delta C_p(T)$ is presented

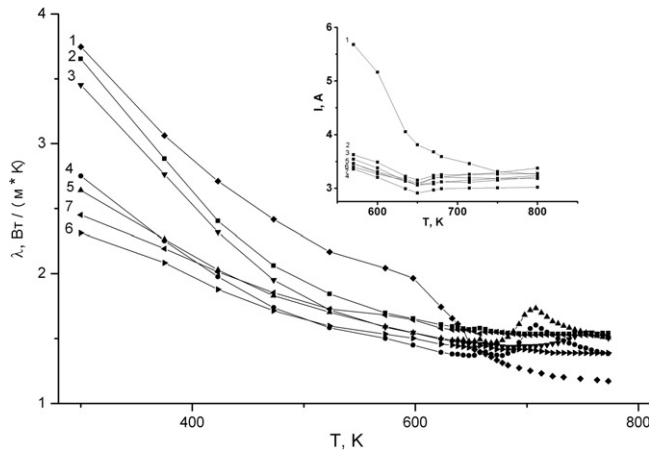


Figure 3. The temperature dependence of thermal conductivity and the mean free path of the phonons $\text{Bi}_{1-x}\text{Pr}_x\text{FeO}_3$ for $x = 0$ (1), 0.05 (2), 0.10 (3), 0.15 (4), 0.20 (5), 0.40 (6) and 0.50 (7).

in Figure 2. The character of the heat capacity determined by this approach allows for interpreting it as the Schottky anomaly for three-level states separated from the ground state by energy barriers E_1 and E_2 . They can be atoms of the same type or the atomic group separated by energy barriers E_1 and E_2 and having three structurally equivalent positions. In the case of doping with rare-earth elements, a three-level system can emerge due to a distortion of the lattice parameters caused by the polar displacements of bismuth and iron ions from the initial positions, and a change in the bond angle between oxygen octahedra FeO_6 [11]. In the general case, the expression for the Schottky heat capacity can be obtained by differentiation of the particle mean energy at the energy levels $C_p = (kT^2)^{-1}(\langle E_i^2 \rangle - \langle E_i \rangle^2)$ [12].

In the case of the three-level model (at arbitrary material mass), the Schottky heat capacity is given as

$$\Delta C_p = \frac{\nu R \left[D_1 (\Delta E_1 / kT)^2 \exp(-\Delta E_1 / kT) + D_2 (\Delta E_2 / kT)^2 \exp(-\Delta E_2 / kT) \right]}{[1 + D_1 \exp(-\Delta E_1 / kT) + D_2 \exp(-\Delta E_2 / kT)]^2}, \quad (1)$$

where D_1 and D_2 are the degeneracy orders of the levels, R is the universal gas constant, and ν is the number of modes [12]. By comparing the heat capacity calculated by Eq. (1) and that found experimentally, the excess heat capacity ΔC_p was obtained for the following model parameters: $D_1 = 131.66$, $D_2 = 8.91$, $E_1 = 0.245$ eV and $E_2 = 0.0986$ eV. There is a sufficiently good agreement between experimental $\Delta C_p(T)$ and calculated temperature dependence of the anomalous heat capacity is (Figure 2). A characteristic λ -anomaly on $C_p(T)$ curve, caused by the appearance of a magnetic ordering was observed near the antiferromagnetic phase transition T_N (Figures 1 and 2).

For compositions with $x = 0.10$, 0.15, and 0.20, the second anomalies at temperatures $T = 755$ K and $T \approx 710$ K, typical for phase transitions, are observed on the curves of thermal conductivity vs temperature (Figure 3), as for the heat capacity (Figure 1) above T_N .

Let us consider the heat transfer mechanism of phonons in the polycrystalline multi-ferroic $\text{Bi}_{1-x}\text{Pr}_x\text{FeO}_3$. The inset in Figure 3 shows the temperature dependence of the

phonon mean free path l , which can be derived from the Debye formula $l = 3\lambda/C_p \cdot v$ (where λ is the thermal conductivity, C_p is the specific heat, and v is the sound velocity [13]). It can be well seen in the inset in Figure 3, the value of l varies from 3 to 5 angstroms. It follows that the mean free path of phonons is much smaller than the dimensions of the crystallites (which are usually of the order of several microns [9]), so that scattering of phonons at crystallite boundaries can be neglected. Thus, it can be assumed that in $\text{Bi}_{1-x}\text{Pr}_x\text{FeO}_3$, structural distortions (scattering centers) limiting the mean free path of phonons, have the order of magnitude of the lattice constant. According to structural studies on neutron diffraction [11], the distortions in the lattice parameters and changes in the volume of the unit cell are attributable to, rotation of oxygen octahedra centers; the angle between the neighboring octahedra of FeO_6 and the polar shifts of bismuth and iron ions from their initial positions increases.

In the temperature region below T_N , the thermal conductivity of the samples increases with decreasing temperature, which is associated with a sharp increase in the mean free path of phonons (see the inset in Figure 3), since the electron-lattice interaction is suppressed by an ordered spin system at the transition to the magnetic phase [14], besides the lattice is compressed [10]. In the temperature region above T_N (Figure 3), the decrease of thermal conductivity of pure BiFeO_3 with heating may be caused by an increase in phonon scattering centers due to lattice distortions [11].

The thermal conductivity of the $\text{Bi}_{1-x}\text{Pr}_x\text{FeO}_3$ system decreasing with increasing concentration x below T_N (see Figure 3) is associated with additional local distortions of the crystalline lattice (i.e., phonon scattering centers) which appear due to the substitution of bismuth ions by praseodymium ions of smaller radius.

The slight substitution of praseodymium for bismuth in polycrystalline bismuth ferrite leads to a marked change in the temperature dependences of the heat capacity and thermal conductivity over a wide range of temperatures, as well as to the temperature shift of the antiferromagnetic transition T_N .

4. Summary

The results of this study demonstrate that the substitution of praseodymium for bismuth results in a marked shifting of the antiferromagnetic phase transition temperature to higher values. The anomalies observed in the temperature dependences of the heat capacity for the compositions with $x = 0.10, 0.15,$ and 0.20 and their analysis in combination with the structural data suggest their cause to be the structural phase transitions. Doping of bismuth ferrite with rare-earth element Pr, brings an additional contribution to the heat capacity in the temperature range of 240–800 K that can be interpreted as the Schottky anomaly for three-level states formed as a result of the distortion of the lattice parameters due to the doping.

References

1. G. A. Smolenskii, and V. M. Yudin, Weak ferromagnetism of some $\text{BiFeO}_3\text{-PbFe}_{0.5}\text{Nb}_{0.5}\text{O}_3$ perovskites. *Sov. Phys. Solid State*. **6**, 2936 (1965).
2. G. Catalan, and F. Scott, Physics and applications of bismuth ferrite. *Adv. Mater.* **21** (24), 2463 (2009). DOI: [10.1002/adma.200802849](https://doi.org/10.1002/adma.200802849).

3. J.-H. Lee *et al.*, Variations of ferroelectric off-centering distortion and 3d – 4p orbital mixing in La-doped BiFeO₃ multiferroics. *Phys. Rev. B.* **82**, 045113 (2010).
4. D. V. Karpinsky *et al.*, Magnetic and piezoelectric properties of the Bi_{1-x}La_xFeO₃ system near the transition from the polar to antipolar phase. *Phys. Solid State.* **56** (4), 701 (2014).
5. D. V. Karpinsky *et al.*, Temperature evolution of the crystal structure of Bi_{1-x}Pr_xFeO₃ solid solutions. *Phys. Solid State.* **56** (11), 2263 (2014). DOI: [10.1134/S1063783414110146](https://doi.org/10.1134/S1063783414110146).
6. D. V. Karpinsky *et al.*, Phase coexistence in Bi_{1-x}Pr_xFeO₃ ceramics. *J. Mater. Sci.* **49** (20), 6937 (2014). DOI: [10.1007/s10853-014-8398-6](https://doi.org/10.1007/s10853-014-8398-6).
7. S. N. Kallaev *et al.*, Heat capacity of multiferroics Bi_{1-x}Pr_xFeO₃. *Phys. Solid State .* **59** (7), 1477 (2017). DOI: [10.1134/S1063783417070095](https://doi.org/10.1134/S1063783417070095).
8. J. Zhang, Y.-J. Wu, and X.-J. Chen, Structural evolution and enhanced magnetization of Bi_{1-x}Pr_xFeO₃. *J. Magn. Mater.* **382**, 1 (2015). DOI: [10.1016/j.jmmm.2015.01.061](https://doi.org/10.1016/j.jmmm.2015.01.061).
9. A. A. Amirov *et al.*, Features of thermal, magnetic, and dielectric properties of the multiferroics BiFeO₃ and Bi_{0.95}La_{0.05}FeO₃. *Phys. Solid State.* **51** (6), 1189 (2009). DOI: [10.1134/S1063783409060183](https://doi.org/10.1134/S1063783409060183).
10. T. Tohei *et al.*, General rule for displacive phase transitions in perovskite compounds revisited by first principles calculations. *Phys. Rev. Lett.* **94**, 035502 (2005).
11. Arnold, D. C. Knight, K. S. Morrison, and F. D. Lightfoot, Ferroelectric-paraelectric transition in BiFeO₃: crystal structure of the orthorhombic β phase. *Phys. Rev. Lett.* **102**, 027602 (2009).
12. R. G. Mitarov *et al.*, Schottky effect in the Pr₃Te₄ - Pr₂Te₃ system. *Phys. Status Solidi A.* **30** (2), 457 (1975).
13. E. P. Smirnova *et al.*, Acoustic properties of multiferroic BiFeO₃ over the temperature range 4.2–830 K. *Eur. Phys. J. B.* **B83**, 39 (2011). DOI: [10.1140/epjb/e2011-20418-1](https://doi.org/10.1140/epjb/e2011-20418-1).
14. H. Fujshiro, S. Sugavara, and M. Ikebe, Proceedings of the 10th international conference on phonon scattering in condensed matter. *Physica B.* **316–317**, 331 (2002). DOI: [10.1016/S0921-4526\(02\)00500-8](https://doi.org/10.1016/S0921-4526(02)00500-8).
15. S. N. Kallaev *et al.*, Heat capacity of BiFeO₃-based multiferroics. *J. Exp. Theor. Phys.* **118** (2), 279 (2014). DOI: [10.1134/S1063776114020095](https://doi.org/10.1134/S1063776114020095).